



FULL $\mathcal{O}(\alpha)$ ELECTROWEAK RADIATIVE CORRECTIONS TO $e^+e^- \rightarrow ZH$ WITH BEAM POLARIZATIONS AT THE ILC

Phan Hong Khiem*, Pham Nguyen Hoang Thinh

University of Science Ho Chi Minh City

Received: 18/12/2017; Revised: 16/01/2018; Accepted: 26/3/2018

ABSTRACT

We present full $\mathcal{O}(\alpha)$ electroweak radiative corrections to $e^+e^- \rightarrow ZH$ with the initial beam polarizations at the International Linear Collider (ILC). The calculation is checked numerically by using three consistency tests that are ultraviolet finiteness, infrared finiteness, and gauge parameter independence. In phenomenological results, we study the impact of the electroweak corrections to total cross section as well as its distributions. In addition, we discuss the possibility of searching for an additional Higgs in arbitrary beyond the Standard Model (BSM) through ZH production at the ILC.

Keywords: Higgs physics at future colliders, numerical method for particle physics, one – loop electroweak corrections, physics beyond the Standard Model.

TÓM TẮT

Các bổ chính bức xạ điện yếu của giản đồ Feynman một vòng cho quá trình $e^+e^- \rightarrow ZH$ với chùm tia tới phân cực tại ILC

Chúng tôi trình bày các bổ chính bức xạ điện yếu của giản đồ Feynman một vòng cho quá trình $e^+e^- \rightarrow ZH$ với chùm tia tới phân cực tại máy gia tốc tuyến tính quốc tế (ILC). Kết quả tính toán được kiểm tra số bằng ba phép kiểm tra: Hữu hạn tử ngoại, hữu hạn hồng ngoại và tính độc lập với các tham số gauge. Trong phần kết quả hiện tượng luận, chúng tôi nghiên cứu về sự ảnh hưởng của các bổ chính điện yếu đối với tiết diện tán xạ và các phân bố tiết diện tán xạ. Hơn nữa, chúng tôi cũng thảo luận về khả năng tìm ra một hạt Higgs (khác với hạt Higgs trong mô hình chuẩn) trong số những mô hình mở rộng của mô hình chuẩn (BSM) thông qua quá trình $e^+e^- \rightarrow ZH$ tại ILC.

Từ khóa: vật lí Higgs tại máy gia tốc tương lai, phương pháp giải số trong vật lí hạt, bổ chính điện yếu của giản đồ Feynman một vòng, vật lí trong các mô hình mở rộng của mô hình chuẩn.

1. Introduction

The discovery of the Standard Model-like Higgs boson at the Large Hadron Collider (LHC) in 2012 [1], [2] has opened up a new era in particle physics which focuses on precision measurement of the Standard Model (SM) as well as search for physics beyond the Standard Model. In particular, one of the main targets of future colliders such as the

* Email: phkiem@hcmus.edu.vn

LHC at high luminosities [3], [4], the ILC [5], is to measure the properties of the Higgs boson. These measurements will be performed at high precision, e.g. the Higgs boson's couplings will be probed at the precision of 1% or better for a statistically significant measurement [5]. This level of precision can be archived at the clean environment of lepton colliders (the ILC as a typical example) rather than hadron colliders. In order to match the high precision data in near future, higher-order corrections to Higgs productions at the ILC are necessary.

The ILC is a proposed e^+e^- -collider including the initial beam polarizations with center of-mass energy (\sqrt{s}) in range of 250 GeV to 500 GeV. The energy can be also expanded up to 1 TeV. The main Higgs production channels at the ILC are Higgsstrahlung (ZH) and WW-, ZZ- fusions. With $250 \text{ GeV} \leq \sqrt{s} \leq 500 \text{ GeV}$, the Higgsstrahlung process is the dominant channel. For the process $e^+e^- \rightarrow ZH$, the advantage of the recoil mass technique [6] can be applied to extract the ZH event which is independent of the Higgs decay channels. Hence, the cross section for this process and its relevant distributions can be measured to few sub-percent accuracy.

Full one-loop electroweak radiative corrections have been computed in Refs. [7] - [9]. In above calculations, the authors have provided the results for polarized leptons as well as polarized Z-boson. However, the detailed numerical investigation for polarizations of e^+, e^- at the ILC, e.g. two beam polarizations which are $(Pe^-, Pe^+) = (-80\%, +30\%)$ and $(+80\%, -30\%)$ have not been presented yet. Recently, mixed electroweak-QCD corrections to this process have been considered in Ref. [10]. The paper has only presented the results for unpolarized beams of e^+, e^- .

In view of the importance of the process $e^+e^- \rightarrow ZH$, we perform the computation again in order to cross-check the previous results, update the physical predictions by using the modern input parameters, and include the initial beam polarizations at the ILC. Moreover, in this paper we develop a model-independent way introducing an additional Higgs boson to the SM. The coupling of the extra Higgs to ZZ which follows the sum rules for Higgs bosons [11]. We then discuss the possibility to probe BSM through ZH production at the ILC.

Our paper is organized as follows: In the next section, we present the calculation in detail. First, the GRACE-LOOP is described briefly. One then performs the numerical checks for the calculation. We next show the physical results for the process $e^+e^- \rightarrow ZH$ with non - polarized beams at the ILC in more detail. In section III, search for the additional Higgs boson at the ILC is discussed. Finally, conclusions and prospects are devoted in section IV.

2. The calculations

In this section, we explain the computation for full one-loop radiative corrections to process $e^+e^- \rightarrow ZH$ in detail. The GRACE program at one-loop [12] used for this computation is described in next subsection.

2.1. GRACE at one loop

GRACE-LOOP is a generic program for the automatic calculation of scattering processes at one-loop electroweak corrections in High Energy Physics. With the complexity of the automatic calculation, the internal consistency checks for the computation are necessary. For this purpose, the program has implemented non-linear gauge fixing terms in the Lagrangian which will be described in the next paragraphs. In GRACE-LOOP, the renormalization has been carried out with the on-shell condition (follows Kyoto scheme) as reported in Ref. [12]. This program has been checked carefully with many of $2 \rightarrow 2$ -body electroweak processes in Ref. [12]. The GRACE-LOOP has also been used to calculate $2 \rightarrow 3$ -body processes such as $e^+e^- \rightarrow ZZH$, $e^+e^- \rightarrow t\bar{t}H$, $e^+e^- \rightarrow \nu\bar{\nu}H$. Moreover, the $2 \rightarrow 4$ -body process as $e^+e^- \rightarrow \nu_\mu\bar{\nu}_\mu HH$ has been performed by using GRACE-LOOP. Recently, full one-loop electroweak radiative corrections to two important processes which are $e^+e^- \rightarrow t\bar{t}\gamma$, $e^+e^- \gamma$ have been computed successfully with the help of the program.

Full one-loop electroweak corrections to a process in the GRACE program are computed as follows. First, we edit a file (it is called `in.prc`) in which the users declare the model (Standard Model in this case), the names of the incoming and outgoing particles, and kinematic configurations for the phase space integration. In the intermediate stage, symbolic manipulation FORM [13] handles all Dirac and tensor algebra in d -dimensions, decomposes the scattering amplitude into coefficients of tensor one-loop integrals and writes the formulas in terms of FORTRAN subroutines on a diagram by diagram basis. The generated FORTRAN code will be combined with libraries which contain the routines that reduce the tensor one-loop integrals into scalar one-loop functions. These scalar functions will be numerically evaluated by one of the FF [14] or LoopTools [15] packages. The ultraviolet divergences (UV-divergences) are regulated by dimensional regularization and the infrared divergences (IR-divergences) is regulated by giving the photon an infinitesimal mass λ . Eventually all FORTRAN routines are linked with the GRACE libraries which include the kinematic libraries and the Monte Carlo integration program BASES [16]. The resulting executable program can finally calculate cross-sections and generate events. Ref [12] describes the method used by the GRACE-LOOP to reduce the tensor one-loop five- and six-point functions into one-loop four-point functions.

As mentioned before, the GRACE-LOOP allows the use of non-linear gauge fixing conditions [12] which are defined as follows

$$\begin{aligned} \mathcal{L}_{GF} = & -\frac{1}{\xi_W} \left| (\partial_\mu - ie\tilde{\alpha}A_\mu - igc_W\tilde{\beta}Z_\mu)W^{\mu+} + \xi_W \frac{g}{2} (v + \tilde{\delta}H + i\tilde{\kappa}_3\chi_3)\chi^+ \right|^2 \\ & - \frac{1}{2\xi_Z} \left(\partial_\mu Z + \xi_Z \frac{g}{2c_W} (v + \tilde{\epsilon}H)\chi_3 \right)^2 - \frac{1}{2\xi_A} (\partial_\mu A)^2. \end{aligned} \quad (1)$$

We work in the R_ξ -type gauges with condition $\xi_W = \xi_Z = \xi_A = 1$ (with so-called the 't Hooft Feynman gauge), there is no contribution of the longitudinal term in the gauge propagator. This choice not only has the advantage of making the expressions much simpler, but also avoids unnecessary large cancellations, high tensor ranks in the one-loop integrals and extra powers of momenta in the denominators which cannot be handled by the FF package.

Recently, we have used our one-loop integral program which has been reported in Ref. [17]. The polarizations for initial beam have been also included in this program [18]. Both new features are used for the calculations in this report.

2.2. $e^+e^- \rightarrow ZH$ with unpolarized beams

The full set of Feynman diagrams with the nonlinear gauge fixing, as described in the previous section, consists of 4 tree diagrams and 341 one-loop diagrams. This includes the counterterm diagrams. In Fig. 1, we show some selected diagrams.

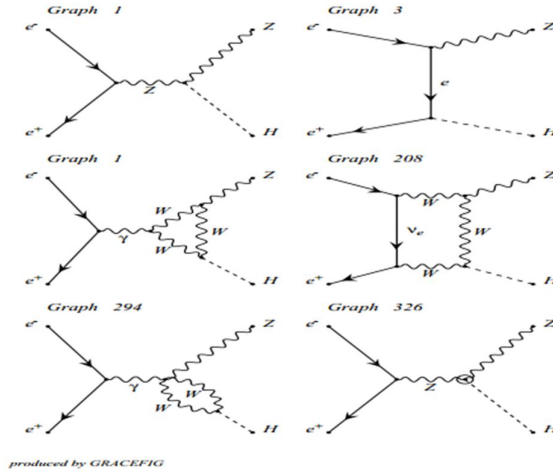


Figure 1. Typical Feynman diagrams for the reaction $e^+e^- \rightarrow ZH$ generated by the GRACE-Loop system

We use the following input parameters for the calculation: The fine structure constant in the Thomson limit is $\alpha^{-1} = 137.0359895$. The mass of the Z boson is taken $M_Z = 91.1876$ GeV and its decay width is $\Gamma_Z = 2.35$ GeV. The mass of the Higgs boson is $M_H = 126$ GeV. In the on-shell renormalization scheme, the mass of W boson is treated as an input parameter. Because of the limited accuracy of the measured value for M_W , we hence take the value that is derived from the electroweak radiative corrections to the muon

decay width (Δr) [12] with $G_\mu = 1.16639 \times 10^{-5} \text{ GeV}^{-2}$. As a result, M_W is a function of M_H . The resulting $M_W = 80.370 \text{ GeV}$ is corresponding to $\Delta r = 2.49\%$. Finally, for the lepton masses we take $m_e = 0.51099891 \text{ MeV}$, $m_\mu = 105.658367 \text{ MeV}$ and $m_\tau = 1776.82 \text{ MeV}$. The quark masses are $m_u = 63 \text{ MeV}$, $m_d = 63 \text{ MeV}$, $m_c = 1.5 \text{ GeV}$, $m_s = 94 \text{ MeV}$, $m_t = 173.5 \text{ GeV}$, and $m_b = 4.7 \text{ GeV}$.

The full $\mathcal{O}(\alpha)$ electroweak cross section considers the tree graphs and the full one-loop virtual corrections as well as the soft and hard bremsstrahlung contributions. In general, the total cross section in full one-loop electroweak radiative corrections is given by

$$\begin{aligned} \sigma_{\mathcal{O}(\alpha)}^{ZH} = & \int d\sigma_T^{ZH} + \int d\sigma_V^{ZH}(C_{UV}, \{\tilde{\alpha}, \tilde{\beta}, \tilde{\delta}, \tilde{\epsilon}, \tilde{\kappa}\}, \lambda) \\ & + \int d\sigma_T^{ZH} \delta_{soft}(\lambda \leq E_{\gamma S} < k_c) + \int d\sigma_H^{ZH}(E_{\gamma S} \geq k_c). \end{aligned} \quad (2)$$

In this formula, σ_T^{ZH} is the tree-level cross section, σ_V^{ZH} is the cross section due to the interference between the one-loop and the tree diagrams. The contribution must be independent of the UV-cutoff parameter (C_{UV}) and the nonlinear gauge parameters ($\tilde{\alpha}, \tilde{\beta}, \tilde{\delta}, \tilde{\epsilon}, \tilde{\kappa}$). Because of the way we regularize the IR divergences, σ_V^{ZH} depends on the photon mass λ . This λ dependence must cancel against the soft-photon contribution, which is the third term in Eq. (2). The soft-photon part can be factorized into a soft factor, which is calculated explicitly in Ref [12], and the cross section from the tree diagrams.

In Tables 1, 2 and 3 in this section, we present the numerical results for the checks of UV finiteness, gauge invariance, and the IR finiteness at one random point in phase space, evaluated with double precision. The results are stable over a range of 14 digits.

Finally, we consider the contribution of the hard photon bremsstrahlung, $\sigma_H^{ZH\gamma S(k_c)}$. This part is the process $e^+e^- \rightarrow ZH\gamma_S$ with an added hard bremsstrahlung photon. The process is generated by the tree-level version of the GRACE [12]. By taking this part into the total cross section, the final results must be independent of the soft-photon cutoff energy k_c . Table 4 shows the numerical result of the check of k_c - stability. Changing k_c from 0.0001 GeV to 0.1 GeV, the results are consistent to an accuracy better than 0.04% (this accuracy is better than that in each Monte Carlo integration).

Table 1. Test of C_{UV} independence of the amplitude. In this table, we take the nonlinear gauge parameters to be (0,0,0,0,0), $\lambda = 10^{-17} \text{ GeV}$ and we use 1 TeV for the center-of-mass energy

C_{UV}	$2\text{Re}(\mathcal{M}_T^* \mathcal{M}_L)$
0	$-8.6563074319085317 \cdot 10^{-2}$
10^2	$-8.6563074319085359 \cdot 10^{-2}$
10^3	$-8.6563074319085234 \cdot 10^{-2}$

Table 2. Test of the IR finiteness of the amplitude. In this table we take the nonlinear gauge parameters to be $(0,0,0,0,0)$, $C_{UV} = 0$ and the center-of-mass energy is 1 TeV.

$\lambda[\text{GeV}]$	$2\text{Re}(\mathcal{M}_T^* \mathcal{M}_L) + \text{soft contribution}$
10^{-15}	$-4.3320229357755305 \cdot 10^{-3}$
10^{-17}	$-4.3320229357753596 \cdot 10^{-3}$
10^{-20}	$-4.3320229357753995 \cdot 10^{-3}$

Table 3. Gauge invariance of the amplitude. In this table, we set $C_{UV} = 0$, the fictitious photon mass is 10^{17} GeV and a 1 TeV center-of-mass energy

$(\tilde{\alpha}, \tilde{\beta}, \tilde{\delta}, \tilde{\epsilon}, \tilde{\kappa})$	$2\text{Re}(\mathcal{M}_T^* \mathcal{M}_L) + \text{soft contribution}$
$(0,0,0,0,0)$	$-8.6563074319085317 \cdot 10^{-2}$
$(1, 2, 3, 4, 5)$	$-8.6563074319085234 \cdot 10^{-2}$
$(10, 20, 30, 40, 50)$	$-8.6563074319075561 \cdot 10^{-2}$

Table 4. Test of the k_c -stability of the result. We choose the photon mass to be 10^{-17} GeV and the center-of-mass energy is 1 TeV. The second column presents the hard photon cross-section and the third column presents the soft photon cross-section. The final column is the sum of both

k_c [GeV]	$\sigma_S \times 10^{-2}$ [pb]	$\sigma_H \times 10^{-2}$ [pb]	$\sigma_{S+H} \times 10^{-2}$ [pb]
10^{-5}	3.291191	2.933921	6.225112
	± 0.002435	± 0.002614	
10^{-4}	3.647297	2.579148	6.226445
	± 0.002698	± 0.002259	
10^{-3}	4.003403	2.220851	6.224254
	± 0.002961	± 0.001956	
10^{-2}	4.359510	1.864859	6.224369
	± 0.003225	± 0.001564	
10^{-1}	4.715616	1.507799	6.223415
	± 0.003488	± 0.001270	

Having verified the stability of the results, we proceed to generate the physical results of the process. Hereafter, we use $\lambda = 10^{-17}$ GeV, $C_{UV} = 0$, $k_c = 10^{-2}$ GeV, and $(\tilde{\alpha}, \tilde{\beta}, \tilde{\delta}, \tilde{\epsilon}, \tilde{\kappa}) = (0,0,0,0,0)$. We defined the percentage of full electroweak radiative corrections as follows:

$$\delta_{EW} [\%] = \frac{\sigma_{O(\alpha)}^{ZH} - \sigma_T^{ZH}}{\sigma_T^{ZH}} \times 100\%. \quad (3)$$

The K_{EW} factor is also shown in the physical results. It is defined as

$$K_{EW} = \frac{\sigma_{\mathcal{O}(\alpha)}^{ZH}}{\sigma_T^{ZH}} - 1. \quad (4)$$

In Fig. 2 (left Figure), we present the total cross section and full electroweak corrections as a function of center-of-mass energy. The energy varies from 220 GeV to 1000 GeV. The cross section has a peak around $\sqrt{s} \approx 250 \text{ GeV} (\approx M_H + M_Z)$. It then decreases when $\sqrt{s} > 250 \text{ GeV}$. On the right corner of this Figure, the percentage of full radiative corrections to the total cross section is shown as a function of \sqrt{s} . We observe that the corrections are from $\approx -40\%$ to $\approx 20\%$ which are corresponding to $220 \text{ GeV} \leq \sqrt{s} \leq 1000 \text{ GeV}$. In the low energy region, QED corrections are dominant. While the weak corrections are the large contribution at higher-energy region. It is well-known that the weak corrections in the high-energy region are attributed to the enhancement contribution of the single Sudakov logarithm. Its contribution can be estimated as follows:

$$\delta_W \approx \frac{\alpha(M_Z^2)}{\pi \sin^2 \theta_W} \ln\left(\frac{s}{M_Z^2}\right) \approx \mathcal{O}(10\%) \quad \text{at } \sqrt{s} = 1000 \text{ GeV}. \quad (5)$$

It is clear that the corrections make a sizable contribution to the total cross section and cannot be ignored for the high-precision program at the ILC.

In Fig. 2 (right Figure), the angular distribution of Z boson is generated at $\sqrt{s} = 250 \text{ GeV}$. In this Figure, the K_{EW} given in Eq. (4) indicates the electroweak corrections to the differential cross section. One finds that the corrections are about $\approx -8\%$. Again, this contribution should be taken into account at the high precision program of the ILC.

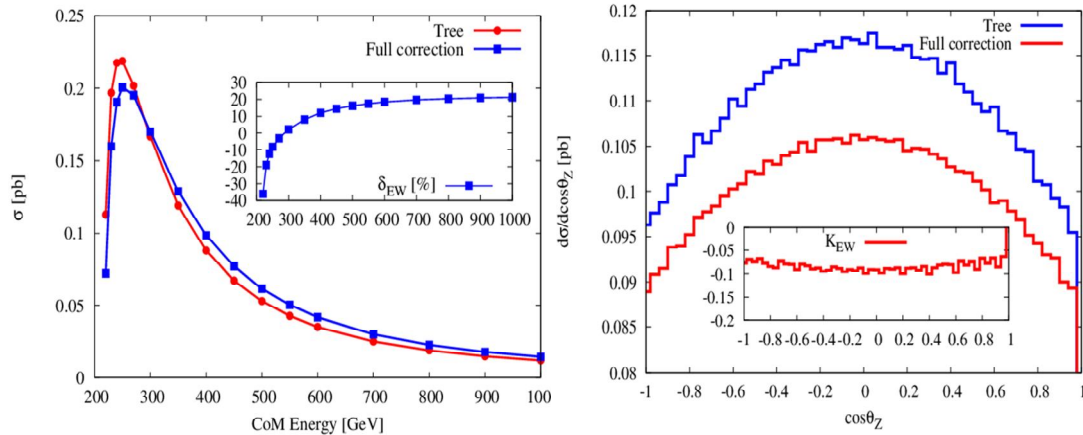


Figure 2. The total cross-section and its distribution

2.3. $e^+e^- \rightarrow ZH$ with polarized beams

The phenomenological results for the reaction $e^+e^- \rightarrow ZH$ including the beam polarizations are shown in this subsection. In GRACE program, the polarizations of electron and positron are implemented by introducing projection operator [18] as follows

$$\sum_{s=1,2} u_{e^-}(p) \bar{u}_{e^-}(p) \frac{1 + \lambda_{e^-} \gamma_5}{2} (\not{p} + m), \quad (6)$$

$$\sum_{s=1,2} u_{e^+}(p) \bar{u}_{e^+}(p) \frac{1 - \lambda_{e^+} \gamma_5}{2} (\not{p} - m). \quad (7)$$

Where $\lambda_{e^-} = \pm 1$ ($\lambda_{e^+} = \pm 1$) are LR for electron (and positron). In this article, we are interested in computing full one-loop electroweak radiative corrections to ZH production with two options of the initial beam polarizations which are $(P_{e^-}, P_{e^+}) = (-80\%, +30\%)$ and $(P_{e^-}, P_{e^+}) = (+80\%, -30\%)$. In general, we use GRACE to generate the following processes

$$e_L^- e_R^+ (e_R^- e_L^+) \rightarrow ZH, \quad (8)$$

$$e_L^- e_L^+ (e_R^- e_R^+) \rightarrow ZH. \quad (9)$$

We know that two latter processes give small cross sections in comparison with the former reactions. Having the cross sections σ_{LR} , σ_{RL} , σ_{LL} and σ_{RR} for this reaction, we then evaluate the cross section at general polarization (P_{e^-}, P_{e^+}) for electron and positron. It is given by

$$\begin{aligned} \sigma(P_{e^-}, P_{e^+}) = & (1 + P_{e^-})(1 + P_{e^+})\sigma_{RR} + (1 - P_{e^-})(1 - P_{e^+})\sigma_{LL} \\ & + (1 - P_{e^-})(1 + P_{e^+})\sigma_{LR} + (1 + P_{e^-})(1 - P_{e^+})\sigma_{RL}. \end{aligned} \quad (10)$$

Of course, after generating all related process by GRACE, we are going to perform the numerical checks as the previous case. The independence of the squared amplitude on the C_{UV} , gauge parameters and λ have been tested. One also confirms that the results are stable over a range of 14 digits. The k_c stability also verified at the cross section level. We obtain that the results are consistent to an accuracy better than 0.02% (this accuracy is better than that in each Monte Carlo integration). After passing the numerical checks, we set the C_{UV} , gauge parameters, λ and k_c back to the default values which have been shown in previous subsection.

We are going to discuss on the physical results for this reaction at the ILC. In Fig. (3), the cross sections at the polarizations for electron, positron which are $(-80\%, +30\%)$ (left panel) and $(+80\%, -30\%)$ (right panel) are shown as a function of center-of-mass energy. Again, we vary the energy from 220 GeV to 1000 GeV. We observe the peaks where the cross sections are maximum, around 250 GeV for both cases. The cross sections in the polarization of $(-80\%, +30\%)$ case are larger than those of $(+80\%, -30\%)$. In these Figures, the K_{EW} are presented for the full electroweak corrections to both cases. For the case of $(-80\%, +30\%)$, one obtains the corrections which vary from $\approx -45\%$ to $\approx 10\%$.

For another case of (+80%, -30%), we find that the corrections change from $\approx -20\%$ to $\approx 40\%$. The corrections in both cases are significant contributions. They play important role at the ILC. The latter case of beam polarizations obtains the larger corrections in high energy regions than former case. They come from the weak correction of vector W boson which couples only to left handed electron.

We concern the differential cross sections which are functions of cosine of Z boson's angle at 250 GeV, as shown in Fig. (4). The left (right) panel is shown for $(P_{e^-}, P_{e^+}) = (-80\%, +30\%)$ and $(+80\%, -30\%)$ respectively. In the first case, the corrections to the differential cross sections are about $\approx -15\%$. For the second case, one obtains that the corrections are $\approx 7.5\%$. In both cases, the corrections are important for future analysis at the ILC.

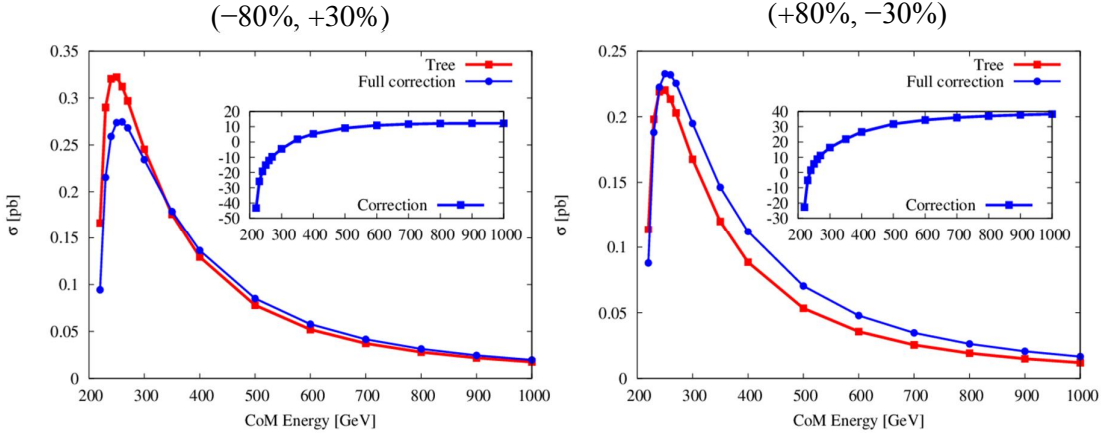


Figure 3. The total cross-section and full electroweak corrections.

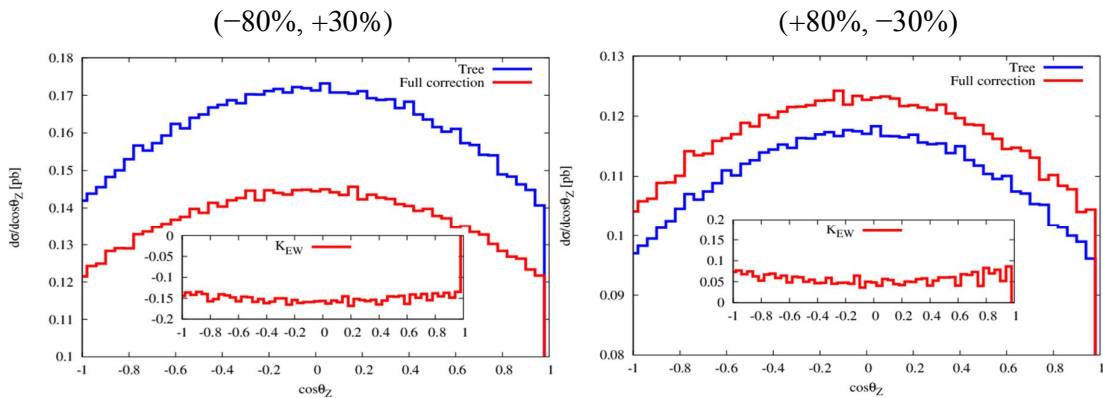


Figure 4. The angular distributions.

3. Search for additional higgs at the ILC

In this section, we are going to discuss on a method to search indirectly the additional Higgs in arbitrary physics beyond the Standard Model. In this model, besides the SM-like Higgs boson (h), we assume that there is an additional Higgs boson (H). We note that the coupling of Standard Model Higgs boson and the additional Higgs boson to ZZ are λ_{hZZ} , λ_{HZZ} respectively. Following the sum rules for Higgs boson [11], these couplings satisfy the below condition

$$\frac{\lambda_{hZZ}^2}{(\lambda_{hZZ}^{\text{SM}})^2} + \frac{\lambda_{HZZ}^2}{(\lambda_{hZZ}^{\text{SM}})^2} = 1, \quad (11)$$

With $\lambda_{hZZ}^{\text{SM}} = \frac{gM_Z}{C_W}$, $C_W = \frac{M_W}{M_Z}$. We know that in the SM $\lambda_{HZZ} = 0$. In this analysis, we vary $0.5 \leq \lambda_{hZZ} \leq 0.95$. It means that the coupling of the additional Higgs boson to ZZ is in the range of $0.31 \leq \lambda_{HZZ} \leq 0.87$. In Fig. (5), the total cross-sections generated with varying $0.5 \leq \lambda_{hZZ} \leq 0.95$ are shown as a function of center-of-mass energy. \sqrt{s} changes from 220 GeV to 1 TeV. The left and right figures present the cross sections for polarizations of initial beam which are $(P_{e^-}, P_{e^+}) = (-80\%, +30\%)$ and $(+80\%, -30\%)$ respectively. In these figures, the red line is for Standard Model case. The blue region is the cross section which the coupling λ_{hZZ} are from 0.5 to 0.9. While the green area shows the cross section corresponding to $\lambda_{hZZ} \in [0.9, 0.95]$. From these analyses, we find that the BSMs effects through this reaction could be tested clearly at the ILC.

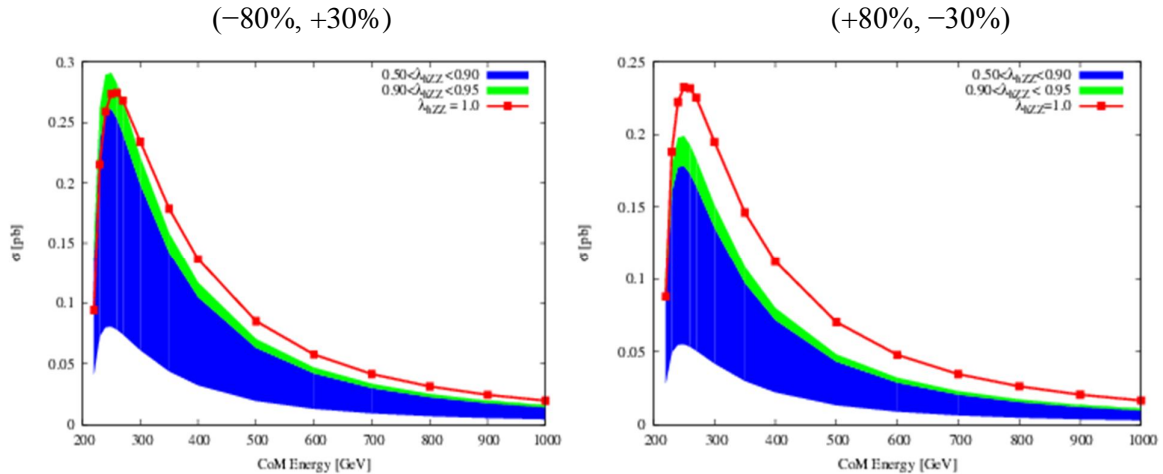


Figure 5. The total cross-section and full electroweak corrections

4. Conclusions

In this article, full $\mathcal{O}(\alpha)$ electroweak radiative corrections to the process $e^+e^- \rightarrow ZH$ at the ILC have been computed successfully. The non-polarized and polarized cases for initial beams have been computed. The radiative corrections are order of 10% contributions to the total cross section as well as its distributions. The corrections are significant contributions and they must be taken into account at the ILC.

We have been also discussed on the model-independent way to probe the additional Higgs in physics of beyond the SM through ZH production at the ILC. With high luminosity program at the ILC, thanks to the full one-loop radiative corrections to this production, we could probe the BSM's effects and may discriminate many of BSMs at the ILC. In future work, we will apply this method for specific BSMs.

❖ **Conflict of Interest:** Authors have no conflict of interest to declare.

❖ **Acknowledgment:** This research is funded by Vietnam National Foundation for Science and Technology Development (NAFOSTED) under grant number 103.01-2016.33.

REFERENCES

- [1] G. Aad et al. [ATLAS Collaboration], "Observation of a new particle in the search for the Standard Model Higgs boson with the ATLAS detector at the LHC," *Phys. Lett. B*, vol. 716, pp. 1-29 (2012), Sept. 2012.
- [2] S. Chatrchyan et al. [CMS Collaboration], "Observation of a new boson at a mass of 125 GeV with the CMS experiment at the LHC," *Phys. Lett. B*, vol. 716, pp. 30-61, Sept. 2012.
- [3] ATLAS Collaboration, "Physics at a High-Luminosity LHC with ATLAS," arXiv:1307.7292 [hep-ex], 2013.
- [4] CMS Collaboration, "Projected Performance of an Upgraded CMS Detector at the LHC and HL-LHC: Contribution to the Snowmass Process," arXiv:1307.7135 [hep-ex], 2013.
- [5] H. Baer et al, "The International Linear Collider Technical Design Report - Volume 2: Physic," arXiv:1306.6352 [hep-ph], 2013.
- [6] J. Yan, S. Watanuki, K. Fujii, A. Ishikawa, D. Jeans, J. Strube, J. Tian and H. Yamamoto, "Measurement of the Higgs boson mass and $e^+e^- \rightarrow ZH$ cross section using $Z \rightarrow \mu^+\mu^-$ and $Z \rightarrow e^+e^-$ at the ILC," *Phys. Rev. D*, vol. 94, no. 11, 113002, Dec. 2016.
- [7] J. Fleischer and F. Jegerlehner, "Radiative corrections to Higgs production by $e^+e^- \rightarrow ZH$ in the Weinberg-Salam model," *Nucl. Phys. B*, vol. 216, pp. 469-492, May 1983.
- [8] B. A. Kniehl, "Radiative corrections for associated ZH production at future e^+e^- colliders," *Z. Phys. C*, vol. 55, pp. 605-618, Dec.1992.

-
- [9] A. Denner, J. Kublbeck, R. Mertig and M. Bohm, “Electroweak radiative corrections to $e^+e^- \rightarrow ZH$,” *Z. Phys. C*, vol. 56, pp. 261–272, June 1992.
- [10] Q.F.Sun, F.Feng, Y.Jia and W.L.Sang, “Mixed electroweak-QCD corrections to $e^+e^- \rightarrow ZH$ at Higgs factories,” *Phys. Rev. D*, vol. 96, no. 5, 051301, Sept. 2017.
- [11] J. F. Gunion, H. E. Haber and J. Wudka, “Sum rules for Higgs bosons,” *Phys. Rev. D*, vol. 43, pp. 904, Feb. 1991.
- [12] G. Belanger, F. Boudjema, J. Fujimoto, T. Ishikawa, T. Kaneko, K. Kato and Y. Shimizu, “Automatic calculations in high energy physics and GRACE at one-loop,” *Phys. Rept.*, vol. 430, pp. 117-209, July 2006.
- [13] J.A.M.Vermaseren, “New Features of FORM,” arXiv:math-ph/0010025 [math-ph], 2000.
- [14] G. J. van Oldenborgh, “FF - a package to evaluate one-loop Feynman diagrams,” *Comput. Phys. Commun*, vol. 66, pp. 1-15, July 1991.
- [15] T. Hahn. (28 Feb 2018). LoopTools. Available: <http://www.feynarts.de/looptools/>.
- [16] S. Kawabata, “A new version of the multi-dimensional integration and event generation package BASES/SPRING,” *Comput. Phys. Commun*, vol. 88, pp. 309-326, Aug. 1995.
- [17] K. H. Phan and T. N. H. Pham, “Scalar one-loop Feynman integrals with complex internal masses revisited,” arXiv:1710.11358 [hep-ph], 2018.
- [18] N. M. U. Quach, Y. Kurihara, K. H. Phan and T. Ueda, “Beam polarization effects on top-pair production at the ILC,” arXiv:1706.03432 [hep-ph], 2017.